

Synchrotron-Like Radiation Beyond The Standard Model I: Hunting for new physics with the Sokolov-Ternov effect

Iftah Galon^{1,*}

¹*New High Energy Theory Center
Rutgers, The State University of New Jersey
Piscataway, New Jersey 08854-8019, USA*

Electron and positron beams in storage-rings self-polarize by emitting spin-flipping synchrotron radiation. If new ultralight particles couple to e^\pm , their emission in synchrotron-like radiation would modify the characteristic self-polarization time. We calculate the rate of spin-flipping synchrotron-like radiation in several simplified models, and find that the largest contribution is for an axial-vector. We use polarization time measurements from the Swiss-Light-Source, and SPEAR3 to set new strong limits on ultralight axial-vectors coupled to e^\pm .

I. INTRODUCTION

Despite its success in describing experimental results up to the TeV-scale, the standard model of particle physics (SM) cannot be a complete theory of Nature. Primary deficiencies of the SM include: the lack of viable dark matter (DM) candidates, an explanation for neutrino oscillations, and an account for the Universe's matter/anti-matter asymmetry. Other issues include the hierarchy problem, the flavor puzzle, and the strong CP puzzle. Theoretical extensions of the SM typically address a subset of these by introducing new degrees of freedom which couple to the SM particles. In such theories, DM candidates characteristically poses interactions, which make them testable in terrestrial experiments, and in non-gravitational astrophysical observations. An interesting class of such new physics (NP) models is that of ultralight DM, with masses lower than ~ 10 eV [1–3]. A yet unexplored avenue is to directly produce such particles in storage-rings.

In storage-rings, an array of electric and magnetic field configurations guides bunches of charged particles in orbits, causing these particles to emit synchrotron radiation. If these particles couple to new physics degrees of freedom, it is conceivable that the latter could also be emitted in *synchrotron-like* radiation. Synchrotron radiation has been widely studied both theoretically and experimentally (see [4–6] for reviews). Some characteristic observables, such as the power spectrum, are understood classically [7], and quantum mechanical effects modify them negligibly [8] for typical storage-ring energies [9]. Nonetheless, particle beams in storage-rings exhibit important effects which are due to the quantum mechanical nature of synchrotron radiation. These effects can therefore constitute a precision test of Quantum Electrodynamics (QED).¹

One such effect is the radiative polarization of electron or positron beams known as the Sokolov-Ternov

(ST) effect [11]. In a storage-ring, the synchrotron induced spin-flip transition rates are asymmetric between the two spin-states. Consequently, polarization builds up over a characteristic (machine-dependent) time scale, up to an asymptotic value. The effect has been extensively verified (see [12–14] for reviews) using beam polarimetry techniques [15]. Uses of the effect include beam energy measurements [16], and the production of polarized-beams in high-energy colliders like LEP [17, 18], and HERA [19, 20].

If new particles couple to electrons, their synchrotron-like radiation modifies the spin-flip transition rates. The aforementioned measurements therefore constrain the parameter-space of new-physics models which couple new light particles to electrons.

This work explores these constraints. A basic review of the ST-effect is presented in Sec. II, and the modifications for real storage-rings are elaborated in Sec. III. Sec. IV discusses the effects of new physics on polarization, describes a set of simplified models, and for each model, presents the “massless”-limit result for the spin-flip transition-rate. The available measurements used in this work are presented in Sec. V and the derived limits are given in Sec. VI. Concluding remarks are given in Sec. VII. The heavy lifting is reserved to the supplemental materials which include a short introduction to spin-dynamics and polarization in accelerator physics, as well as the technical details of the formalism, approximation methods, and the full results of the calculations.

II. THE SOKOLOV-TERNOV EFFECT - RADIATIVE SELF POLARIZATION OF CHARGED PARTICLES IN STORAGE-RINGS

In a storage ring with a uniform and constant background magnetic field, relativistic electrons and positrons emit synchrotron radiation which either flips or preserves their spin state. Due to the magnetic field, the spin-flip transition-rates,

$$\Gamma_\gamma^{\text{sf}}(u) \equiv \Gamma_H(e^-(u) \rightarrow e^-(-u)\gamma), \quad (1)$$

*Electronic address: iftah.galon@physics.rutgers.edu

¹ synchrotron-like production can also act as a DM-source [10].

depend on the fermion spin state, $u = +, -$ for “up“ and “down” along the magnetic field direction respectively (\hat{z}). The polarization of the beam is the average

$$\mathcal{P} = \frac{1}{N} \sum_{i=1}^N \langle \vec{S}_i \cdot \hat{z} \rangle = \frac{N_+ - N_-}{N_+ + N_-} \quad (2)$$

where the sum runs over the N particle spins, and N_{\pm} is the number of particles in each respective spin state ($N = N_+ + N_-$). The state population is governed by the rates in Eq. (1) using a transport equation

$$\frac{d}{dt} \begin{pmatrix} N_+ \\ N_- \end{pmatrix} = \begin{pmatrix} -\Gamma_{\gamma}^{\text{sf}}(+), & \Gamma_{\gamma}^{\text{sf}}(-) \\ \Gamma_{\gamma}^{\text{sf}}(+), & -\Gamma_{\gamma}^{\text{sf}}(-) \end{pmatrix} \begin{pmatrix} N_+ \\ N_- \end{pmatrix}. \quad (3)$$

For an initially unpolarized beam this leads to

$$\mathcal{P}(t) = \mathcal{P}_{eq} \left(1 - e^{-t/\tau_p} \right). \quad (4)$$

where the equilibrium polarization and the characteristic polarization time are respectively

$$\mathcal{P}_{eq} = \frac{\Gamma_{\gamma}^{\text{sf}}(+)-\Gamma_{\gamma}^{\text{sf}}(-)}{\Gamma_{\gamma}^{\text{sf}}(+)+\Gamma_{\gamma}^{\text{sf}}(-)} \quad \tau_p^{-1} = \Gamma_{\gamma}^{\text{sf}}(+)+\Gamma_{\gamma}^{\text{sf}}(-). \quad (5)$$

Sokolov and Ternov calculate $\Gamma_{\gamma}^{\text{sf}}(u)$ in a constant and uniform background magnetic field, H , [11] (see also [21]). In natural units,² their result for electrons reads

$$\Gamma_{\gamma}^{\text{sf}}(u) \Big|_{ST} = e^2 \frac{E_i}{m\rho} \frac{5\sqrt{3}}{144\pi} \left(1 + \frac{8}{5\sqrt{3}}u \right) \xi_0^2, \quad (6)$$

where e is the QED coupling, E_i is the beam energy, m is the electron mass, and ρ is the radius of a circular and planar storage-ring, $eH = \beta E_i/\rho \approx E_i/\rho$. The parameter,

$$\xi_0 \equiv \frac{\frac{3}{2}eHE_i}{m^3}, \quad (7)$$

characterizes the importance of quantum effects in synchrotron radiation. In storage-rings, $\xi_0 \ll 1$ as terrestrial magnetic fields are small (in natural units).³ Using Eq. (5) one finds [4, 9, 11, 13, 24–26]

$$\begin{aligned} |\mathcal{P}_{eq}| \Big|_{ST} &\equiv |\mathcal{P}_{ST}| = \frac{8}{5\sqrt{3}} \approx 92.4\% \\ \tau_p \Big|_{ST} &\equiv \tau_{ST} = \left(e^2 \frac{E_i}{m\rho} \frac{5\sqrt{3}}{72\pi} \xi_0^2 \right)^{-1}. \end{aligned} \quad (8)$$

The spins of an electron beam tend to align anti-parallel to the magnetic field. Positron beams do the reverse, a result obtained by taking $u \rightarrow -u$ in Eq. (6).

III. MODIFICATIONS OF THE SOKOLOV-TERNOV EFFECT IN REAL STORAGE-RINGS

A. Effective Radius

Realistic storage-ring designs are not circles with a uniform and constant magnetic field. Typical designs have both straight and curved sections, respectively known as *insertions* and *arcs*, with bending magnetic fields predominantly in the latter. This modifies the circular ring radius, ρ , in Eq. (8) to an effective radius [24] given by

$$\rho_{\text{eff}} = \left(\frac{\oint |\rho(s)|^{-3} ds}{\oint ds} \right)^{-1/3} = (\rho^2 R)^{-1/3} \quad (9)$$

where $\rho(s)$ is the bending radius as a function of the ring contour parameterization, s . The last equality is for a ring consisting of insertions ($\rho \rightarrow \infty$), and arcs of equal and constant bending radius ρ , and circumference given by $2\pi R$, where R is the effective geometric radius. Additional modifications occur for the equilibrium polarization which also take into account the direction of the magnetic field in each arc [27].

B. Real Beam Optics

Machine deliverables require an intricate system of non-uniform and time-dependent electromagnetic field configurations resulting in the so called “beam-optics” [25, 28]. Some facilities also include a series of insertion devices like wigglers and undulators which increase synchrotron-radiation production rates or focus them to specific frequencies [29, 30]. The emission of synchrotron radiation in such environments induces a natural depolarization effect known as “spin-diffusion” [9, 13, 25, 26, 31]. The ST-polarization and spin-diffusion-depolarization are competing effects, which typically result in a lower asymptotic polarization, and shorter polarization time. A detailed discussion is given in the supplemental materials. For the “quiet” planar rings we consider in this work, and given a set of machine running conditions which are away from spin-orbit resonances [32–34], the quantities in Eq. (4) are modified to [27, 35]

$$\mathcal{P}_{eq} = \mathcal{P}_{ST} \frac{\tau_p}{\tau_{ST}} + \mathcal{P}_{kin}, \quad \tau_p^{-1} = \tau_d^{-1} + \tau_{ST}^{-1}. \quad (10)$$

The term \mathcal{P}_{kin} is called the “kinetic polarization”, and is typically very small for planar rings (see [35], and the supplemental material).

In “quiet” rings, the characteristic depolarization time, τ_d , is very long, and the polarization observables come very close to the Sokolov-Ternov prediction. New physics contributions are therefore constrained so as to not modify these results. Moreover, if both the polarization and

² Here we apply a the conventional particle-physics system of “natural units”, with $\hbar = c = 1$.

³ This is not the case for example in pulsars [22, 23] and other astrophysical systems.

the polarization time are measured, then their ratio,

$$\frac{\mathcal{P}_{eq}}{\tau_p} = \frac{\mathcal{P}_{ST}}{\tau_{ST}}, \quad (11)$$

can be used to constrain various new physics contributions. In practice, the time measurement resolution is superior to that of the asymptotic beam polarization, and the τ_p measurements put stronger constraints.

IV. NEW PHYSICS EFFECTS ON POLARIZATION OBSERVABLES

The polarization time in Eq. (10) would be modified by the synchrotron-like spin-flipping emission of an ultralight DM particle, X ,

$$\tau_p^{-1} = \tau_d^{-1} + \tau_{ST}^{-1} + \tau_X^{-1}. \quad (12)$$

In order to calculate X 's contribution to the polarization time, τ_X^{-1} , we follow in the footsteps of Sokolov & Ternov's original calculation using the "method of exact solutions" approach. We perform a perturbation theory expansion using exact solutions of the Dirac equation in a uniform, and constant background magnetic field [11]. The derivation is lengthy, and is therefore kept to the supplemental materials, where we generalize the ST approach in order to take into account massive particles.

Notably, other approaches lead to the same results for the photon case, but are not straightforward to generalize to the massive case. For QED, the use of a *semi-classical effective Hamiltonian* approach [24, 35] is easier to apply in realistic magnetic field configurations. The formalism of [36, 37] is useful for the massive case as well.⁴

A. Simplified Models

We consider four simplified models in which a new particle X couples to electrons. In these models $X = \{V^\mu, A^\mu, S, a\}$, i.e. a massive vector, an axial vector, a scalar, and a pseudo-scalar. The interaction Lagrangians are given by

$$\mathcal{L}_{\text{int}} \supset g_V \bar{\psi} \gamma^\mu \psi V_\mu, \quad g_A \bar{\psi} \gamma^\mu \gamma^5 \psi A_\mu, \quad g_S \bar{\psi} \psi S, \quad i g_a \bar{\psi} \gamma^5 \psi a \quad (13)$$

where canonically normalized kinetic terms, and mass terms, are implicit.

B. X -Induced Spin-Flip Rates

Following the notations of Sec. II, we calculate the transition-rate for an initial state electron to emit a

X -particle, such that the final state electron spin has flipped,

$$\Gamma_X^{\text{sf}} \equiv \Gamma_H(e^-(u) \rightarrow e^-(-u)X). \quad (14)$$

For a massive X , these rates are attenuated when the value of the "phase-space" parameter, $\frac{m_X}{m \xi_0}$ exceeds unity. The full results are given as differential transition rates in the supplemental material, and have to be numerically integrated. While we employ them in this analysis, it is instructive to explore the "massless" limit, $\frac{m_X}{m \xi_0} \rightarrow 0$, for which Γ_X^{sf} is maximized. In this limit, the calculation can be performed analytically, and presented as an expansion in ξ_0 . We find,

$$\Gamma_{V_T}^{\text{sf}} = g_V^2 \frac{5\sqrt{3}}{144\pi} \frac{E_i}{m\rho} \left(1 + \frac{8}{5\sqrt{3}}u\right) \xi_0^2 \quad (15)$$

$$\Gamma_{V_L}^{\text{sf}} = g_V^2 \frac{5\sqrt{3}}{144\pi} \frac{E_i}{m\rho} \left(\frac{m^2 m_V^2}{108 E_i^4}\right) \left(1 + \frac{8}{5\sqrt{3}}u\right) \xi_0^2 \quad (16)$$

$$\Gamma_{A_T}^{\text{sf}} = g_A^2 \frac{1}{144\pi} \frac{E_i}{m\rho} \left(36(\sqrt{3} + u)\right) \quad (17)$$

$$\Gamma_{A_L}^{\text{sf}} = g_A^2 \frac{\sqrt{3}}{162\pi} \frac{E_i}{m\rho} \left(85 + 48\sqrt{3}u\right) \frac{m^2}{4m_A^2} \xi_0^2 \quad (18)$$

$$\Gamma_S^{\text{sf}} = g_S^2 \frac{5\sqrt{3}}{162\pi} \frac{E_i}{m\rho} \xi_0^2 \quad (19)$$

$$\Gamma_a^{\text{sf}} = g_a^2 \frac{\sqrt{3}}{162\pi} \frac{E_i}{m\rho} \left(85 + 48\sqrt{3}u\right) \xi_0^2 \quad (20)$$

where for the massive vector, and axial-vector cases we distinguish between the transverse, and longitudinal modes, denoting them by T , and L respectively.

A few points are noteworthy here. First, our result for $\Gamma_{V_T}^{\text{sf}}$ agrees with the ST one, see Eq. (6). Second, the results for the longitudinal modes behave as expected. In the axial-vector case, $\Gamma_{A_L}^{\text{sf}} = \left(\frac{m^2}{4m_A^2}\right) \Gamma_a^{\text{sf}}$, which is consistent with the Goldstone Boson Equivalence theorem. In the vector case, $\Gamma_{V_L}^{\text{sf}}$ has the correct decoupling properties [39], but otherwise preserves the spin-flip structure of the transverse mode. Third, while scalars in a magnetic field can flip the spin, the flip rate is insensitive to the spin-state, and so polarization does not build up overall.⁵ Most importantly, with the exception of $\Gamma_{A_T}^{\text{sf}}$, all the spin-flip rates start at the ξ_0^2 order! We stress that the previous statement also includes $\Gamma_{A_L}^{\text{sf}}$ which is enhanced [40], but subject to the unitarity constraint [41, 42]

$$g_A \frac{m}{m_A} \lesssim \sqrt{\frac{\pi}{2}}. \quad (21)$$

The lack of ξ_0 (magnetic field) suppression in the transverse axial-vector spin-flip rate arises due to its spin-parity quantum numbers. It can be readily understood

⁴ [38] applies these methods to calculate Weak gauge-boson synchrotron emission, but incorrectly excludes the Goldstone boson contribution from the loop. Nonetheless, the rates are negligible.

⁵ In fact, for a scalar, all $u \rightarrow u'$ transitions have the same rate.

by noting that in the non-relativistic limit, an axial-vector couples directly to the electron spin.

The experimental precision for polarization measurements is at the sub-to few-percent level [15]. If Γ_X^{sf} is at the same order in ξ_0 as the SM contribution, then the corresponding X sensitivity would not be competitive with existing searches. We therefore focus on the *axial-vector* case [43].

V. AVAILABLE EXPERIMENTAL RESULTS

Beam polarization measurements have been performed in a plethora of machines with energies in the range ~ 0.5 GeV – 45 GeV [12–14]. We focus on “quiet” low-energy storage-rings, such as third-generation synchrotron light-sources. These are particularly interesting because the machine running conditions can be tuned to have negligible depolarization effects, such that the polarization-time nearly saturates the Sokolov-Ternov prediction. Table I presents the polarization measurements used in this work. The last column, gives a conservative 2σ estimate for the sum of depolarization effects:

$$\Gamma_X^{\text{max}} = (\tau_p - 2\Delta\tau_p)^{-1} - \tau_{ST}^{-1}, \quad (22)$$

which is used in Sec. VI for limit setting. While other measurements exist (for example [46–52]), we prioritize those which have the highest precision, and provide standard errors on fit parameters.

The SLS [44], and SPEAR3 [45] measurements employ the resonant spin-depolarization technique [53, 54], a standard beam polarimetry technique which is often used for accurate calibration of the beam energy. In resonant spin-depolarization, a radio-frequency magnetic field is turned on in the plane of the ring. The frequency of the field is set to a spin resonance, an integer times $a_e\gamma$ [33], which causes the beam to depolarize. When the field is turned-off, the beam begins to polarize again. Due to the Touschek effect [55, 56]⁶ the beam lifetime is correlated with its polarization, and τ_p can be measured by monitoring beam losses as those decrease after the beam has been depolarized. Note that this technique only measures τ_p , while P_{eq} is deduced assuming the SM, i.e. assuming the ST-effect (though see [57]). In addition, the dependence of the Touschek scattering on the beam polarization is not modified by an additional weakly coupled axial-vector force that mediates the reaction.

Other polarimetry techniques exist with potentially higher precision [15]. We mention in passing the

Compton backscattering based polarimeters [58]⁷, including the Fabry-Perot cavity used in the final days of HERA [20]. These two techniques measure the polarization directly, rather than just its relative build-up over time. We refrain from using these measurements in this work. To the best of our knowledge, the inverse-Compton-based methods were not used in sufficiently “quiet” machines, while the HERA measurements were done at relatively high-energy, with large depolarization effects.

VI. EXPERIMENTAL REACH

Limits on new axial-vectors coupled to electrons are set by requiring that their contribution to the spin-flip rate does not exceed the sum of all depolarizing contributions which is estimated by Eq. (22),

$$\Gamma_X^{\text{sf}} < \Gamma_X^{\text{max}} \quad (23)$$

The discussion of Sec. III A is taken into account by applying a global rescaling factor, ρ/R to the Γ_X^{sf} full results for (see also Eqs. (17) and (18)). Fig. 1 shows the resulting limits in the $\{g_A, m_A\}$ plane. Notably, these strong limits represent a conservative estimate as they assume negligible machine induced depolarization effects. We point out that τ_d could be estimated using dedicated algorithms and tracking codes [34, 59–68] to a 10% accuracy [69] which in turn, would lead to stronger limits.

While the SLS and SPEAR3 facilities have $\xi_0 \sim 2 \times 10^{-6}$, the SLS limit is stronger due to a quieter environment, and a more precise measurement (Table I). In addition, both limits are stronger than the unitarity requirement, Eq. (21). The reach is dominated by the longitudinal-mode contribution up to the $\xi_0 m \approx 1$ eV scale where phase-space effects come into play, and the transverse mode contributions (dashed) become comparable.

The limits obtained here are model independent, and require only that a spin-1 particle couples to e^\pm through an axial-vector coupling. In concrete models with a spin-1 particle, a vector coupling imposes additional constraints [39, 71–73]. Some of these constraints may also apply directly to the axial-vector couplings, however, such an analysis is beyond the scope of this work. Interestingly, 5th-force experiments and equivalence-principle tests [74] are not sensitive to axial-couplings because the low-energy potential induced by an axial-vector couples spins, and therefore averages to zero. Notwithstanding, black-hole superradiance signatures [70] may limit the axial-vector coupling directly. Moreover, if the

⁶ Intra-beam collisions (Møller scattering) of oppositely polarized electrons have a higher cross-section and therefore lead to a higher beam loss rate (particles emitted out of the beam).

⁷ Coherent laser scattering off the beam exhibits polarization dependent energy and detector-plane hit distributions. By monitoring this over time, the polarization observables, Eq. (10), can be measured.

Exp	E_i [GeV]	ρ [m]	$2\pi R$ [m]	ξ_0	τ_{ST}	τ_p	Γ_X^{\max} [GeV]
SLS [44]	2.4	11.48	288	2.22×10^{-6}	1873 sec	1837 ± 1 sec	7.478×10^{-30}
SPEAR3 [45]	3.0	8.144	234.144	2.44×10^{-6}	1003 sec	840 ± 17 sec	1.605×10^{-28}

TABLE I: Summary of experimental data on beam polarization measurements used in this work.

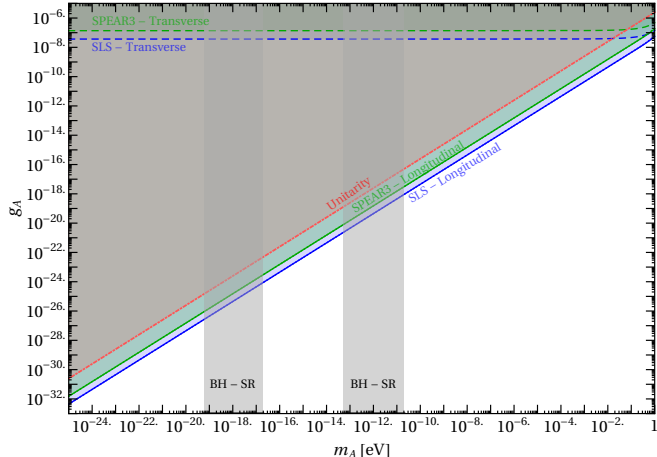


FIG. 1: Limits on light axial-vectors coupled to electrons in the $\{g_A, m_A\}$ plane. Shaded regions are excluded. The triangular exclusion (constrained by the red dotted-dashed line) corresponds to the unitarity constraint of Eq. (21). The two gray bands correspond to limits from black hole super-radiance (BH-SR) [70]. Other possible limits are referred to in the text. The SLS and SPEAR3 constraints are given in blue and green respectively. Dashed lines correspond to the transverse contributions, while the continuous ones are the sum of the transverse and longitudinal ones.

longitudinal mode of the axial-vector is interpreted as an axion-like particle, then additional bounds may exist from the corresponding searches [2, 75, 76]. Finally, this analysis is complementary to [77], which constrains Z' -models down to $\mathcal{O}(10 \text{ eV})$ using atomic parity violation experiments.

VII. CONCLUSIONS AND OUTLOOK

The Sokolov-Ternov effect, the radiative self-polarization of e^\pm -beams, is a well tested phenomenon in storage-rings.⁸ Synchrotron-like emission of new light particles off e^\pm can modify polarization observables, and is therefore testable using polarization measurement. In “quiet” storage-rings, depolarization effects are small,

⁸ See [78, 79] for recent storage-ring based direct-detection experiments

and polarization measurements are sufficiently accurate to constitute as precision tests of the effect.

This work explores the sensitivity of these measurements to new physics. We calculate the spin-flip transition-rates following the Sokolov-Ternov approach, by generalizing the “method of exact solutions”, and the associated approximations to include massive particles. We find that the characteristic polarization time is particularly sensitive to spin-flips by axial-vectors which are not suppressed by the smallness of laboratory magnetic fields, in contrast to particles with other spin-parity assignments.

Limits are set by requiring that the axial-vector contribution to the polarization time does not exceed that of the measured sum of depolarization effects. This conservative approach results in extremely strong limits on light axial-vectors coupled to electrons. Nonetheless, there is potential for improvement by applying dedicated storage-ring tracking tools which can reliably estimate the depolarization effects, namely, τ_d .

Acknowledgments

I am grateful to Tom Banks, Matt Buckley, Ranny Budnik, Jeff Dror, Marat Freytsis, Yuri Gershtein, Enrique Kajomovitz, Simon Knapen, Zohar Komargodski, Stefan Schmitt, Yael Shadmi, David Shih, Yotam Soreq, and Scott Thomas, for the many fruitful discussions which have benefited this work. I am particularly grateful to Desmond Barber, for a careful read of the manuscript, and for many fruitful discussions. Most of all, I am grateful to my family for their support in these challenging and uncertain times. This work was supported in part by DOE grant DE-SC0010008.

References

- [1] R. Essig *et al.*, “Working Group Report: New Light Weakly Coupled Particles,” in *Community Summer Study 2013: Snowmass on the Mississippi*. 10, 2013. [arXiv:1311.0029 \[hep-ph\]](#).
- [2] M. Battaglieri *et al.*, “US Cosmic Visions: New Ideas in Dark Matter 2017: Community Report,” in *U.S. Cosmic Visions: New Ideas in Dark Matter*. 7, 2017. [arXiv:1707.04591 \[hep-ph\]](#).
- [3] J. Redondo and A. Ringwald, “Light shining through walls,” *Contemp. Phys.* **52** (2011) 211–236, [arXiv:1011.3741 \[hep-ph\]](#).
- [4] Sokolov, A.A. and Ternov, I.M., *RADIATION FROM RELATIVISTIC ELECTRONS*. American Institute of Physics, Translation Series, 1986.

- [5] H. Wiedemann, *Theory of Synchrotron Radiation*. Springer Berlin Heidelberg, Berlin, Heidelberg, 2003.
- [6] A. Hofmann, *The Physics of Synchrotron Radiation*. Cambridge Monographs on Particle Physics, Nuclear Physics and Cosmology. Cambridge University Press, 2004.
- [7] J. S. Schwinger, “On the classical radiation of accelerated electrons,” *Phys. Rev.* **75** (1949) 1912.
- [8] J. Schwinger, “THE QUANTUM CORRECTION IN THE RADIATION BY ENERGETIC ACCELERATED ELECTRONS,” *Proceedings of the National Academy of Sciences* **40** (1954) no. 2, 132–136. <https://www.pnas.org/content/40/2/132>.
- [9] A. Chao, “Polarization of a stored electron beam,” *AIP Conf. Proc.* **87** (1982) 395–449.
- [10] I. Galon, “Work in progress.”
- [11] A. Sokolov and I. Ternov, “On polarization and spin effects in the theory of synchrotron radiation,” *Sov. Phys. Dokl.* **8** (1964) no. 12, 1203–1205.
- [12] Y. Shatunov, “Polarized beams at storage rings,” *Phys. Part. Nucl. Lett.* **3** (2006) S1–S6.
- [13] S. Mane, Y. Shatunov, and K. Yokoya, “Spin-polarized charged particle beams in high-energy accelerators,” *Rept. Prog. Phys.* **68** (2005) 1997–2265.
- [14] E. Gianfelice-Wendt, “Self-Polarization in Storage Rings,” *PoS SPIN2018* (2018) 013.
- [15] K. Aulenbacher, E. Chudakov, D. Gaskell, J. Grames, and K. D. Paschke, “Precision electron beam polarimetry for next generation nuclear physics experiments,” *Int. J. Mod. Phys. E* **27** (2018) no. 07, 1830004.
- [16] G. Fischer, D. Gustavson, J. Johnson, J. Murray, T. Phillips, R. Prepost, R. Schwitters, C. K. Sinclair, and D. Wisner, “ENERGY CALIBRATION OF SPEAR BY g -2 PRECESSION,”
- [17] L. Knudsen, J. Koutchouk, M. Placidi, R. Schmidt, M. Crozon, J. Badier, A. Blondel, and B. Dehning, “First observation of transverse beam polarization in LEP,” *Phys. Lett. B* **270** (1991) 97–104.
- [18] G. Alexander, G. Altarelli, A. Blondel, G. Coignet, E. Keil, D. E. Plane, and D. Treille, “POLARIZATION AT LEP.2,”
- [19] D. Barber *et al.*, “The HERA polarimeter and the first observation of electron spin polarization at HERA,” *Nucl. Instrum. Meth. A* **329** (1993) 79–111.
- [20] **POL2000** Collaboration, B. Sobloher, “Polarisation and Polarimetry at HERA,” [arXiv:1201.3836 \[physics.ins-det\]](https://arxiv.org/abs/1201.3836).
- [21] V. C. Zhukovskii, A. A. Sokolov, I. M. Ternov, and B. V. Kholomai, “Quantum theory of the motion of relativistic electrons in an axisymmetric magnetic field of a focusing type,” *Theoretical and Mathematical Physics* **6** (1971) no. 1, 56–62. <https://doi.org/10.1007/BF01037579>.
- [22] V. Skobelev, “Primakoff effect: Synchrotron and Coulomb mechanisms of axion emission,” *Phys. Atom. Nucl.* **63** (2000) 1963–1968.
- [23] A. Borisov and V. Grishina, “Axion synchrotron emission: A New bound on the axion - electron coupling constant,” *J. Exp. Theor. Phys.* **79** (1994) 837–839.
- [24] J. D. Jackson, “On Understanding Spin-Flip Synchrotron Radiation and the Transverse Polarization of Electrons in Storage Rings,” *Rev. Mod. Phys.* **48** (1976) 417–433.
- [25] A. W. Chao and M. Tigner, *Handbook of Accelerator Physics and Engineering*. World Scientific, Singapore, 1st edition, 3rd printing ed., 2006. <https://cds.cern.ch/record/384825>.
- [26] D. Barber, “Introduction to Spin Polarisation in Accelerators and Storage Rings,” (2006) . https://www.desy.de/~mpybar/psdump/Redone_CI_lectures_2006.pdf.
- [27] V. N. Baier, V. M. Katkov, and V. M. Strakhovenko, “Kinetics of Radiative Polarization,” *Sov. Phys. JETP* **31** (1970) 908–911.
- [28] H. Wiedemann, *Introduction to Accelerator Physics*. Springer International Publishing, 2015.
- [29] D. H. Bilderback, P. Elleaume, and E. Weckert, “Review of third and next generation synchrotron light sources,” *Journal of Physics B: Atomic, Molecular and Optical Physics* **38** (apr, 2005) S773–S797.
- [30] M. Couprie, “New generation of light sources: Present and future,” *Journal of Electron Spectroscopy and Related Phenomena* **196** (2014) 3 – 13. Advances in Vacuum Ultraviolet and X-ray Physics, The 38th International Conference on Vacuum Ultraviolet and X-ray Physics (VUVX2013), University of Science and Technology of China.
- [31] D. Barber and G. Ripken, “Radiative polarization, computer algorithms and spin matching in electron storage rings,” [arXiv:physics/9907034](https://arxiv.org/abs/physics/9907034).
- [32] M. Froissart and R. Stora, “Depolarization of a beam of polarized protons in a synchrotron,” *Nucl. Instrum. Meth.* **7** (1960) 297–305.
- [33] V. Baier and Y. Orlov, “QUANTUM DEPOLARIZATION OF ELECTRONS IN A MAGNETIC FIELD,” *Sov. Phys. Dokl.* **10** (1966) 1145.
- [34] D. Barber, J. Ellison, and K. Heinemann, “Quasiperiodic spin-orbit motion and spin tunes in storage rings,” *Phys. Rev. ST Accel. Beams* **7** (2004) 124002, [arXiv:physics/0412157](https://arxiv.org/abs/physics/0412157).
- [35] Y. Derbenev and A. Kondratenko, “Polarization kinematics of particles in storage rings,” *Sov. Phys. JETP* **37** (1973) 968–973.
- [36] J. S. Schwinger and W.-Y. Tsai, “Radiative polarization of electrons,” *Phys. Rev. D* **9** (1974) 1843–1845.
- [37] W.-Y. Tsai and A. Yildiz, “Motion of an electron in a homogeneous magnetic field-modified propagation function and synchrotron radiation. (erratum),” *Phys. Rev. D* **8** (1973) 3446. [Erratum: Phys.Rev.D 9, 2489 (1974)].
- [38] P. Chen and R. J. Noble, “Electroweak Synchrotron Radiation,” *SLAC-PUB-3842* (12, 1985) .
- [39] H. An, M. Pospelov, and J. Pradler, “New stellar constraints on dark photons,” *Phys. Lett. B* **725** (2013) 190–195, [arXiv:1302.3884 \[hep-ph\]](https://arxiv.org/abs/1302.3884).
- [40] J. A. Dror, R. Lasenby, and M. Pospelov, “Light vectors coupled to bosonic currents,” *Phys. Rev. D* **99** (2019) no. 5, 055016, [arXiv:1811.00595 \[hep-ph\]](https://arxiv.org/abs/1811.00595).
- [41] F. Kahlhoefer, K. Schmidt-Hoberg, T. Schwetz, and S. Vogl, “Implications of unitarity and gauge invariance for simplified dark matter models,” *JHEP* **02** (2016) 016, [arXiv:1510.02110 \[hep-ph\]](https://arxiv.org/abs/1510.02110).
- [42] J. A. Dror, “Discovering leptonic forces using nonconserved currents,” *Phys. Rev. D* **101** (2020) no. 9, 095013, [arXiv:2004.04750 \[hep-ph\]](https://arxiv.org/abs/2004.04750).
- [43] Y. Kahn, G. Krnjaic, S. Mishra-Sharma, and T. M. P. Tait, “Light Weakly Coupled Axial Forces: Models,

- Constraints, and Projections,” *JHEP* **05** (2017) 002, [arXiv:1609.09072](https://arxiv.org/abs/1609.09072) [hep-ph].
- [44] S. Leemann, M. Boege, M. Dehler, V. Schlott, and A. Streun, “Precise beam energy calibration at the SLS storage ring,” in *8th European Particle Accelerator Conference (EPAC 2002)*, pp. 662–664. 6, 2002.
- [45] K. Wootton *et al.*, “Storage ring lattice calibration using resonant spin depolarization,” *Phys. Rev. ST Accel. Beams* **16** (2013) no. 7, 074001.
- [46] C. Steier, J. Byrd, and P. Kuske, “Energy calibration of the electron beam of the ALS using resonant depolarization,” in *7th European Particle Accelerator Conference (EPAC 2000)*, pp. 1566–1568. 6, 2000.
- [47] I. Birkel, E. Huttel, A.-S. Muller, M. Pont, F. Perez, and R. Rossmanith, “Energy Calibration of the ANKA Storage Ring,” in *9th European Particle Accelerator Conference (EPAC 2004)*. 7, 2004.
- [48] C. Sun, J. Li, S. Mikhailov, V. Popov, W. Wu, Y. Wu, A. Chao, H.-l. Xu, and J.-f. Zhang, “Electron Beam Polarization Measurement using Touschek Lifetime Technique,” *Conf. Proc. C* **100523** (2010) MOPEA080.
- [49] P. Kuske, P. Schmid, R. Gorgen, and J. Kuszynski, “Improvements of the Set-up and Procedures for Beam Energy Measurements at BESSY II,” *Conf. Proc. C* **100523** (2010) MOPD083.
- [50] J. Zhang, L. Cassinari, M. Labat, A. Nadji, L. Nadolski, and D. Pedeau, “Precise beam energy measurement using resonant spin depolarization in the SOLEIL storage ring,” *Nucl. Instrum. Meth. A* **697** (2013) 1–6.
- [51] N. Carmignani, F. Ewald, L. Farvacque, B. Nash, and P. Raimondi, “Modeling and Measurements of Spin Depolarization,” in *6th International Particle Accelerator Conference*, p. MOPWA013. 2015.
- [52] N. Vitoratou, P. Karataev, and G. Rehm, “Continuous energy measurement of the electron beam in the storage ring of Diamond Light Source with resonant spin depolarization,” *Phys. Rev. Accel. Beams* **22** (2019) no. 12, 122801.
- [53] V. Baier, “RADIATIVE POLARIZATION OF ELECTRONS IN STORAGE RINGS,” *Soviet Physics Uspekhi* **14** (Jun, 1972) 695–714. <https://doi.org/10.1070%2Fpu1972v014n06abeh004751>.
- [54] Y. Derbenev, A. Kondratenko, S. Serebnyakov, A. Skrinsky, G. Tumaikin, and Y. Shatunov, “ACCURATE CALIBRATION OF THE BEAM ENERGY IN A STORAGE RING BASED ON MEASUREMENT OF SPIN PRECESSION FREQUENCY OF POLARIZED PARTICLES,” *Part. Accel.* **10** (1980) 177–180.
- [55] C. Bernardini, G. Corazza, G. Di Giugno, G. Ghigo, R. Querzoli, J. Haissinski, P. Marin, and B. Touschek, “Lifetime and beam size in a storage ring,” *Phys. Rev. Lett.* **10** (1963) 407–409.
- [56] A. Streun, “Beam Lifetime in the SLS Storage Ring,” , Swiss Light Source, Paul Scherrer Institute, 2001.
- [57] T. Lee, J. Choi, and H. Kang, “Simple determination of Touschek and beam-gas scattering lifetimes from a measured beam lifetime,” *Nucl. Instrum. Meth. A* **554** (2005) 85–91.
- [58] D. Gustavson, J. Murray, T. Phillips, R. Schwitters, C. K. Sinclair, J. Johnson, R. Prepost, and D. Wisler, “A Back Scattered Laser Polarimeter for e^+e^- Storage Rings,” *Nucl. Instrum. Meth.* **165** (1979) 177.
- [59] A. Chao, “Evaluation of Radiative Spin Polarization in an Electron Storage Ring,” *Nucl. Instrum. Meth.* **180** (1981) 29.
- [60] K. Yokoya, “Calculation of equilibrium electron polarization using a tracking code,” *Int. J. Mod. Phys. Proc. Suppl. A* **2B** (1993) 1103–1105.
- [61] Y. Eidelman and V. Yakimenko, “SPINLIE: New computer code for polarization calculation,” *Conf. Proc. C* **930517** (1993) 450–453.
- [62] K. Heinemann and G. Hoffstaetter, “A Tracking algorithm for the stable spin polarization field in storage rings using stroboscopic averaging,” *Phys. Rev. E* **54** (1996) 4240–4255, [arXiv:acc-physics/9605001](https://arxiv.org/abs/acc-physics/9605001).
- [63] K. Yokoya, “An Algorithm for calculating the spin tune in circular accelerators,” [arXiv:physics/9902068](https://arxiv.org/abs/physics/9902068).
- [64] A. Luccio, A. Lehrach, J. Niederer, T. Roser, M. Syphers, and N. Tsoupas, “New capabilities of the spin tracking code SPINK,” in *IEEE Particle Accelerator Conference (PAC 99)*, pp. 1578–1580. 3, 1999.
- [65] S. Mane, “MILES: A new nonperturbative formalism to calculate the invariant spin field in circular accelerators,” *Nucl. Instrum. Meth. A* **498** (2003) 1–15.
- [66] K. Heinemann, D. P. Barber, J. A. Ellison, and M. Vogt, “A detailed and unified treatment of spin-orbit systems using tools distilled from the theory of bundles,” [arXiv:1501.02747](https://arxiv.org/abs/1501.02747) [physics.acc-ph].
- [67] D. T. Abell, D. Meiser, V. H. Ranjbar, and D. P. Barber, “Accurate and efficient spin integration for particle accelerators,” *Phys. Rev. ST Accel. Beams* **18** (2015) 024001, [arXiv:1501.03450](https://arxiv.org/abs/1501.03450) [physics.acc-ph].
- [68] Z. Duan, M. Bai, D. P. Barber, and Q. Qin, “A Monte-Carlo simulation of the equilibrium beam polarization in ultra-high energy electron (positron) storage rings,” *Nucl. Instrum. Meth. A* **793** (2015) 81–91, [arXiv:1505.02392](https://arxiv.org/abs/1505.02392) [physics.acc-ph].
- [69] D. Barber, “Private communication,”.
- [70] M. Baryakhtar, R. Lasenby, and M. Teo, “Black Hole Superradiance Signatures of Ultralight Vectors,” *Phys. Rev. D* **96** (2017) no. 3, 035019, [arXiv:1704.05081](https://arxiv.org/abs/1704.05081) [hep-ph].
- [71] M. Goodsell, J. Jaeckel, J. Redondo, and A. Ringwald, “Naturally Light Hidden Photons in LARGE Volume String Compactifications,” *JHEP* **11** (2009) 027, [arXiv:0909.0515](https://arxiv.org/abs/0909.0515) [hep-ph].
- [72] S. Knapen, T. Lin, and K. M. Zurek, “Light Dark Matter: Models and Constraints,” *Phys. Rev. D* **96** (2017) no. 11, 115021, [arXiv:1709.07882](https://arxiv.org/abs/1709.07882) [hep-ph].
- [73] J. Redondo, “Atlas of solar hidden photon emission,” *JCAP* **07** (2015) 024, [arXiv:1501.07292](https://arxiv.org/abs/1501.07292) [hep-ph].
- [74] M. B. Wise and Y. Zhang, “Lepton Flavorful Fifth Force and Depth-dependent Neutrino Matter Interactions,” *JHEP* **06** (2018) 053, [arXiv:1803.00591](https://arxiv.org/abs/1803.00591) [hep-ph].
- [75] G. Raffelt, *Stars as laboratories for fundamental physics: The astrophysics of neutrinos, axions, and other weakly interacting particles*. 5, 1996.
- [76] A. Ringwald, “Axions and Axion-Like Particles,” in *49th Rencontres de Moriond on Electroweak Interactions and Unified Theories*, pp. 223–230. 2014. [arXiv:1407.0546](https://arxiv.org/abs/1407.0546) [hep-ph].
- [77] G. Arcadi, M. Lindner, J. Martins, and F. S. Queiroz, “New Physics Probes: Atomic Parity Violation, Polarized Electron Scattering and Neutrino-Nucleus Coherent Scattering,” [arXiv:1906.04755](https://arxiv.org/abs/1906.04755) [hep-ph].

- [78] P. W. Graham, S. Haciomeroglu, D. E. Kaplan, Z. Omarov, S. Rajendran, and Y. K. Semertzidis, “Storage Ring Probes of Dark Matter and Dark Energy,” [arXiv:2005.11867](https://arxiv.org/abs/2005.11867) [[hep-ph](https://arxiv.org/abs/2005.11867)].
- [79] R. Janish and H. Ramani, “Muon $g-2$ and EDM experiments as muonic dark matter detectors,” [arXiv:2006.10069](https://arxiv.org/abs/2006.10069) [[hep-ph](https://arxiv.org/abs/2006.10069)].
- [80] G. Hoffstaetter, “High-energy polarized proton beams: A modern view,” *Springer Tracts Mod. Phys.* **218** (2006) 1–177.
- [81] B. W. Montague, “Polarized Beams in High-energy e^+e^- Storage Rings,” *Phys. Rept.* **113** (1984) 1–96.
- [82] L. H. Thomas, “I. the kinematics of an electron with an axis,” *The London, Edinburgh, and Dublin Philosophical Magazine and Journal of Science* **3** (1927) no. 13, 1–22.
- [83] V. Bargmann, L. Michel, and V. Telegdi, “Precession of the polarization of particles moving in a homogeneous electromagnetic field,” *Phys. Rev. Lett.* **2** (1959) 435–436.
- [84] Y. Derbenev and A. Kondratenko, “Diffusion of particle spins in storage elements,” *Sov. Phys. JETP* **35** (1972) 230.
- [85] D. E. Aspnes, “Electric-Field Effects on Optical Absorption near Thresholds in Solids,” *Phys. Rev.* **147** (1966) 554–566.

Supplemental Material

Iftah Galon

I. POLARIZATION AND SPIN DYNAMICS IN STORAGE RINGS

Spin dynamics and polarization in accelerator physics is an intricate topic. This section summarizes key points which are used in this work. The interested reader is referred to reviews by [13, 80], and to the useful lecture notes by [26].

In accelerator physics, particle dynamics is governed by an accelerator Hamiltonian. If the electromagnetic fields are sufficiently spatially homogeneous, Stern-Gerlach forces can be neglected, which implies that the spin does not back-react on the orbital dynamics. In these cases, the general form of the quantum Hamiltonian can be written as [13, 80]

$$\hat{\mathcal{H}} = \hat{\mathcal{H}}_{orb} + \hat{W} \cdot \hat{S} \quad (S1)$$

where \mathcal{H}_{orb} is the Hamiltonian for the orbital dynamics, and \vec{S} is the quantum spin operator, defined in the rest frame of the particle (hats denote operators). In the semi-classical approximation approach the Ehrenfest theorem is applied (see also [26]) to obtain an equation of motion for the *classical spin-vector*, $\vec{s} = \langle \hat{S} \rangle$,

$$\frac{d\vec{s}}{dt} = \vec{\Omega} \times \vec{s} \quad (S2)$$

where a ‘‘classical’’ trajectory is assumed, i.e. $\vec{\Omega} = \langle \hat{W}(\hat{q}, \hat{p}) \rangle \approx \vec{W}(\langle \vec{q} \rangle, \langle \vec{p} \rangle)$. This is a good approximation for most low-energy storage rings as the characteristic orbital times are much shorter than those for the spin polarization, see [26, 81]. For spin-physics, the orbital phase space can be considered *ergodic*. In the case of single particle dynamics, in constant and uniform electromagnetic fields, the Ω in Eq. (S2) is given by the Thomas-Bargmann-Michel-Telegdi equation [82, 83],

$$\Omega_{TBMT} = -\frac{e}{m} \left[\left(a + \frac{1}{\gamma} \right) \vec{B} - \frac{a\gamma}{\gamma+1} (\beta \cdot \vec{B}) \vec{\beta} - \left(a + \frac{1}{\gamma+1} \right) \vec{\beta} \times \vec{E} \right] \quad (S3)$$

The approximation breaks down when radiation is involved because the time-scale for radiation emission is much shorter than any orbital time-scale. To take radiation into account one uses the *semi-classical effective Hamiltonian for QED* approach [24, 35]. The effective single-particle Hamiltonian is obtained by extending the background field interactions to the radiation fields,⁹ i.e.

$$\hat{\mathcal{H}}_{semi-classical \text{ QED}} = \left((\hat{p} - e\hat{A})^2 + m^2 \right)^{1/2} + e\hat{V} + \hat{\Omega} \cdot \hat{S}. \quad (S4)$$

Here the electromagnetic field dependent terms are denoted as (hatted) operators because they involve both the background (classical) field, and the quantized radiation field (operator),

$$\vec{A} = \vec{A}^{bkg} + \vec{A}^{rad}, \quad V = V^{bkg} + V^{rad}, \quad \vec{\Omega} = \vec{\Omega}^{bkg} + \vec{\Omega}^{rad} \quad (S5)$$

and the Hamiltonian can be expanded in powers of the radiation field.

The asymmetry in the spin-flip transition rates contributes to polarization build up. In equilibrium, the beam polarization, generally written as $\vec{\mathcal{P}} = \frac{1}{N} \sum_{i=1}^N \langle \vec{s}_i \rangle$, can be written as the average [13, 27, 35, 53, 84]

$$|\vec{\mathcal{P}}_{eq}| = | \langle \langle \vec{s} \cdot \hat{n} \rangle \hat{n} \rangle | = \frac{\langle \Gamma_+ - \Gamma_- \rangle}{\langle \Gamma_+ + \Gamma_- \rangle} \quad (S6)$$

⁹ Alternatively, by a Foldy-Wouthuysen transformation [26]

The vector $\hat{n} = \hat{n}(z, \theta)$, known as the *invariant spin-field* [80], is a field of spin-quantization axes on the generalized phase-space point, $z = z(\vec{q}, \vec{p})$, and generalized azimuthal coordinate along the ring. The invariant spin-field is a solution of Eq. (S2), required to be one-turn periodic. Namely, after one turn, i.e. $\theta \rightarrow \theta + 2\pi$, a particle phase-space location evolves from its initial phase-space point, z_i , to z_f , a new phase-space location. The requirement on \hat{n} is expressed as

$$\mathcal{M}\hat{n}(z, \theta) = \hat{n}(\mathcal{M}z, \theta) \quad (\text{S7})$$

where \mathcal{M} performs the evolution of the system in the spin, and orbital spaces, and is known as the *one-turn spin-orbital map* [13, 80]. In Eq. (S6) the spin projection onto the quantization-axis is averaged over the local phase-space volume element at z (inner average), and the outer average is over the entire orbital phase-space. This is then expressed as a balance of spin-flip transition rates. In the second equality, the averages are of spin-flip transition rates over the entire orbital phase-space.

Derbenev and Kondratenko [35, 84] show how to perform the averages in Eq. (S6), taking into account general electromagnetic field configurations using the invariant spin-field,

$$\mathcal{P}_{DK} = \mathcal{P}_{ST} \frac{\langle \oint ds \frac{1}{|\rho|^3} \hat{b} \cdot (\hat{n} - \frac{\partial \hat{n}}{\partial \delta}) \rangle}{\langle \oint ds \frac{1}{|\rho|^3} \left(1 - \frac{2}{9} (\hat{n} \cdot \hat{v})^2 + \frac{11}{18} \left| \frac{\partial \hat{n}}{\partial \delta} \right|^2 \right) \rangle} \quad (\text{S8})$$

$$\tau_{DK}^{-1} = \tau_{ST}^{-1} \langle \oint ds \frac{1}{|\rho|^3} \left(1 - \frac{2}{9} (\hat{n} \cdot \hat{v})^2 + \frac{11}{18} \left| \frac{\partial \hat{n}}{\partial \delta} \right|^2 \right) \rangle \quad (\text{S9})$$

where $\hat{b} = \frac{\hat{v} \times \dot{\hat{v}}}{|\hat{v} \times \dot{\hat{v}}|}$, \hat{v} is a unit vector in the direction of the local velocity, $\dot{\hat{v}}$ is its time-derivative, and s is a length element along the storage ring. The average is performed on the orbital phase-space (z). The $\frac{\partial}{\partial \delta}$ derivatives are with respect to $\delta = \Delta p/p$, the relative momentum offset, one of the orbital-phase space coordinates.

In most “quiet” planar rings, the product $\hat{n} \cdot \hat{v}$ is negligible. Neglecting $\hat{n} \cdot \hat{v}$ terms in Eqs. (S8) and (S9), and defining

$$\mathcal{P}_{kin} = -\mathcal{P}_{ST} \frac{\tau_{DK}}{\tau_{ST}} \langle \oint ds \frac{1}{|\rho|^3} \hat{b} \cdot \frac{\partial \hat{n}}{\partial \delta} \rangle, \quad \tau_d^{-1} = \tau_{ST}^{-1} \langle \oint ds \frac{1}{|\rho|^3} \frac{11}{18} \left| \frac{\partial \hat{n}}{\partial \delta} \right|^2 \rangle, \quad (\text{S10})$$

one obtains Eq. (10). In “quiet”, planar rings, \hat{n} is close to vertical, and $\partial \hat{n} / \partial \delta$ is small. As a result, the kinetic polarization is small!

In a photon emission process, the initial and final charged particle states have different energies (E_i , and E_f respectively). As a result, the spin quantization axes of the initial state, $|n(E_i)\rangle$, and the final state, $|n(E_f)\rangle$ are misaligned, and the initial and final fermion states are not orthogonal. With this observation, Derbenev and Kondratenko conclude that the spin-flip transition rate draws from two contributions in the semi-classical QED effective theory Eq. (S4). The first is the spin-dependent term, $\vec{\Omega}_{rad} \cdot \vec{s}$, and the second is from the usual covariant derivative term. The latter, is typically diagonal in the spin sub-space, but due to the misalignment of the spin-quantization axes it can non-trivially couple the initial and final spin-states. While this effect is sub-leading with respect to the spin-conserving photon emission, it is of the same order of magnitude as that coming from the $\vec{\Omega}_{rad} \cdot \vec{s}$ term.

For new physics with a direct spin-dependent coupling at leading order, as in the case of an axial-vector, a similar effect would be sub-leading, and so we ignore its possible contributions.

II. NOTATIONS AND CONVENTIONS

Greek letters are used to denote space-time indices running over 0, 1, 2, 3. Roman letters are used to denote space indices running over 1, 2, 3. The space-time Minkowski metric is chosen with mostly negative signature

$$g_{\mu\nu} = \text{diag}[1, -1, -1, -1] \quad (\text{S11})$$

For the Dirac γ -matrices we use the Chiral representation:

$$\gamma^\mu = \begin{pmatrix} 0 & \sigma^\mu \\ \bar{\sigma}^\mu & 0 \end{pmatrix} \quad (\text{S12})$$

where $\sigma^\mu = (1_{2X2}, \sigma^i)$, and $\bar{\sigma}^\mu = (1_{2X2}, -\sigma^i)$ are four-vectors of $2X2$ matrices, σ^i are the Pauli matrices which are given by,

$$\sigma^1 = \begin{pmatrix} 0 & 1 \\ 1 & 0 \end{pmatrix}, \quad \sigma^2 = \begin{pmatrix} 0 & -i \\ i & 0 \end{pmatrix}, \quad \sigma^3 = \begin{pmatrix} 1 & 0 \\ 0 & -1 \end{pmatrix}. \quad (\text{S13})$$

Explicitly,

$$\gamma^0 = \begin{pmatrix} 0 & 0 & 1 & 0 \\ 0 & 0 & 0 & 1 \\ 1 & 0 & 0 & 0 \\ 0 & 1 & 0 & 0 \end{pmatrix}, \quad \gamma^1 = \begin{pmatrix} 0 & 0 & 0 & 1 \\ 0 & 0 & 1 & 0 \\ 0 & -1 & 0 & 0 \\ -1 & 0 & 0 & 0 \end{pmatrix}, \quad \gamma^2 = \begin{pmatrix} 0 & 0 & 0 & -i \\ 0 & 0 & i & 0 \\ 0 & i & 0 & 0 \\ -i & 0 & 0 & 0 \end{pmatrix}, \quad \gamma^3 = \begin{pmatrix} 0 & 0 & 1 & 0 \\ 0 & 0 & 0 & -1 \\ -1 & 0 & 0 & 0 \\ 0 & 1 & 0 & 0 \end{pmatrix}, \quad \gamma^5 = \begin{pmatrix} -1 & 0 & 0 & 0 \\ 0 & -1 & 0 & 0 \\ 0 & 0 & 1 & 0 \\ 0 & 0 & 0 & 1 \end{pmatrix} \quad (\text{S14})$$

The four-vector derivative operator is given by

$$\partial_\mu = \frac{\partial}{\partial x^\mu} = \left(\frac{\partial}{\partial x^0}, \vec{\nabla} \right) \quad (\text{S15})$$

the kinetic four-momentum representation is given by $p^\mu = i\partial^\mu$. The spin-matrices are given by

$$\Sigma^k = \begin{pmatrix} \sigma^k & 0 \\ 0 & \sigma^k \end{pmatrix} \quad (\text{S16})$$

III. DIRAC EQUATION SOLUTION IN A BACKGROUND CONSTANT & UNIFORM MAGNETIC FIELD, IN CYLINDRICAL COORDINATES

We consider Quantum Electrodynamics with an external background magnetic field as the unperturbed theory. For this theory the Lagrangian is given by

$$\mathcal{L} = \bar{\psi} \left(i\cancel{\partial} - eQA^{\text{bkg}} - m \right) \psi - \frac{1}{4} F^{\mu\nu} F_{\mu\nu} \quad (\text{S17})$$

In this theory, momentum is conserved only along the z -axis. The Dirac field can be quantized using the wave function solutions to the E.O.M's with positive-energy (particle) and negative-energy (anti-particle) states. These wave function solutions are given by

$$\psi_{\epsilon_p}(r, \phi, z, t) = \exp(-i\epsilon_p E t) \frac{\exp(i\epsilon_p k_3 z)}{\sqrt{L}} \frac{\exp(i(\ell - \frac{1}{2})\phi)}{\sqrt{2\pi}} \exp(-i\frac{1}{2}\phi\Sigma_3) \sqrt{2\gamma} \begin{pmatrix} c_1 \mathcal{I}_{n-1,s}(\rho) \\ c_2 \mathcal{I}_{n,s}(\rho) \\ c_3 \mathcal{I}_{n-1,s}(\rho) \\ c_4 \mathcal{I}_{n,s}(\rho) \end{pmatrix} \quad (\text{S18})$$

where we have defined,

$$\gamma = \frac{1}{2} eQH, \quad \rho = \gamma r^2 \quad (\text{S19})$$

and where $\epsilon_p = \pm$ for particle/anti-particle, and Q is the corresponding charge in units of $(-e)$. For the z -axis we take a one-dimensional box with edges at $\pm L$, which can later be taken to infinity. The Lagurre gaussian functions are¹⁰

$$\mathcal{I}_{n,s}(\rho) = \sqrt{\frac{1}{n!s!}} e^{-\rho/2} \rho^{\frac{n-s}{2}} Q_s^{n-s}(\rho) \quad (\text{S20})$$

where $n - s = \ell$ is a positive integer called the **Landau-level**, ℓ, s are integers, and the Q functions are the Lagurre polynomials. The c_i 's are chosen such that $\sum_i |c_i|^2 = 1$, and ψ is chosen as an eigenstate, such that

$$\frac{m}{\sqrt{E^2 - k_3^2}} \mu_3 \psi = u\psi, \quad u = \pm 1 \quad (\text{S21})$$

¹⁰ Note that these are properly normalized, i.e. $\int_0^\infty (\mathcal{I}_{n,s}(\rho))^2 = 1$

where μ_3 is the magnetic polarization in the 3-direction which is defined by

$$\mu_3 = \Sigma^3 - i\epsilon^{3,j,k}\gamma^j \frac{P^k}{m} \quad (\text{S22})$$

here $P = p + eA^{bkg}$ is the canonical momentum.

$$\begin{aligned} c_1^{\epsilon_p} &= \frac{1}{2} \left(1 - \frac{k_3}{E}\right)^{1/2} \left(1 + \frac{mu}{\sqrt{E^2 - k_3^2}}\right)^{1/2} & c_3^{\epsilon_p} &= +\frac{1}{2}u \epsilon_p \left(1 + \frac{k_3}{E}\right)^{1/2} \left(1 + \frac{mu}{\sqrt{E^2 - k_3^2}}\right)^{1/2} \\ c_2^{\epsilon_p} &= -\frac{i}{2} \epsilon_p \left(1 + \frac{k_3}{E}\right)^{1/2} \left(1 - \frac{mu}{\sqrt{E^2 - k_3^2}}\right)^{1/2} & c_4^{\epsilon_p} &= +\frac{i}{2}u \left(1 - \frac{k_3}{E}\right)^{1/2} \left(1 - \frac{mu}{\sqrt{E^2 - k_3^2}}\right)^{1/2} \end{aligned} \quad (\text{S23})$$

The energy eigenvalues are given by

$$E \equiv E_{n,k_3} = (m^2 + k_3^2 + 4\gamma n)^{1/2} \quad (\text{S24})$$

IV. FIELD QUANTIZATION

The Dirac field is quantized such that,

$$\psi(t, r, \phi, z) = \int \frac{dk_3}{2\pi\sqrt{2E_{n,k_3}}} \sum_{n,s,u=\pm 1} \frac{e^{i\ell\phi}}{\sqrt{2\pi}} \left(e^{-i(E_{n,k_3}t - k_3z)} U(n, s, k_3, u) a_{n,s,k_3,u} + e^{+i(E_{n,k_3}t - k_3z)} V(n, s, k_3, u) b_{n,s,k_3,u}^\dagger \right) \quad (\text{S25})$$

where U and V are the *radial* four component spinor wave-functions from Eq. (S18),

$$\begin{cases} U \\ V \end{cases} = \sqrt{2E_{n,k_3}} \sqrt{2\gamma} e^{-i\frac{\phi}{2}(1_4 \times 4 + \Sigma_3)} \begin{pmatrix} c_1^\pm \mathcal{I}_{n-1,s}(\rho) \\ c_2^\pm \mathcal{I}_{n,s}(\rho) \\ c_3^\pm \mathcal{I}_{n-1,s}(\rho) \\ c_4^\pm \mathcal{I}_{n,s}(\rho) \end{pmatrix}, \quad (\text{S26})$$

and c_i 's are taken from Eq. (S23) with $\epsilon_p = +1, -1$ for U, V respectively. Note that with this normalization $\int_0^\infty dr r^2 \{U^\dagger U, V^\dagger V\} = 2E_{n,k_3}$. States are normalized such that

$$\begin{aligned} \sqrt{2E_{n,k_3}} a_{n,s,k_3,u}^\dagger |0\rangle &= |1_{\text{particle}}, n, s, k_3, u\rangle \\ \sqrt{2E_{n,k_3}} b_{n,s,k_3,u}^\dagger |0\rangle &= |1_{\text{anti-particle}}, n, s, k_3, u\rangle \\ a_{n,s,k_3,u} |0\rangle &= b_{n,s,k_3,u} |0\rangle = 0 \end{aligned} \quad (\text{S27})$$

where the corresponding creation/annihilation operators obey the anti-commutation relations

$$\{a_{n,s,k_3,u}^\dagger, a_{n',s',k'_3,u'}\} = \{b_{n,s,k_3,u}^\dagger, b_{n',s',k'_3,u'}\} = \delta_{nn'} \delta_{ss'} \delta_{k_3 k'_3} \delta_{uu'} \quad (\text{S28})$$

and with all other anti-commutators vanishing. These result in

$$\{\psi(r, \phi, z), \psi^\dagger(r', \phi', z')\} = 1_{4 \times 4} \frac{1}{r} \delta(r - r') \delta(z - z') \delta(\phi - \phi') \quad (\text{S29})$$

The choice of the ‘‘particle physics’’ field normalization factor ($2E_{n,k_3}$) is to assure a Lorentz invariant form to boosts along the 3-direction.

For the $X = \{V^\mu, A^\mu, S, a\}$ radiation fields we use free particle solutions. For V^μ

$$V_\mu(x, t) = \int \frac{d^3q}{(2\pi)^3} \frac{1}{\sqrt{2E_q}} \sum_{r=0}^3 (a_q^r \epsilon_\mu^r(q) e^{-ix \cdot q} + a_q^{r\dagger} \epsilon_\mu^{r*}(q) e^{+ix \cdot q}) \quad (\text{S30})$$

and with similar expressions for the other fields.

V. THE X -EMISSION RATE

The calculation of the X -emission rate involves *four* small parameter expansions. The first is the usual small coupling series expansion of time-dependent perturbation theory. This is discussed in Sec. V A. The second, is an expansion of the reduced matrix element in terms of several characteristically small kinematic ratios. This is discussed in Sec. V B. The third, is a WKB approximation of the Lagurre-Gaussian functions, $\mathcal{I}_{n,n'}(\bar{x})$ close to the turning point, where $1 - \bar{x}/x_0$ is small. This is discussed in Sec. V C. In the final evaluation step, it is useful to expand the results as a power series in ξ_0 from Eq. (7). The following subsections closely follow [4], and generalize its results and analyses to the massive X case.

A. X -emission in first-order perturbation theory

X -emission is described in first-order perturbation theory by the interaction Lagrangian

$$\mathcal{L}_{\text{int}} = \int d^3x \bar{\psi}(\vec{x}, t) O_X(\vec{x}, t) \psi(\vec{x}, t) \quad (\text{S31})$$

where O_X is an operator linear in the X -field, with a model dependent spinor representation. The initial and final states are respectively,

$$\begin{aligned} |i\rangle &= \sqrt{2E_{n,k_3}} |1_{\text{particle}}, n, s, k_3, u\rangle, \\ |f\rangle &= \sqrt{2E_{n',k'_3}} |1_{\text{particle}}, n', s', k'_3, u'\rangle \times \sqrt{2E_q} |1_X, \vec{q}\rangle \end{aligned} \quad (\text{S32})$$

where the X 3-momentum, \vec{k} , is chosen in the YZ -plane using the azimuthal symmetry of the problem,

$$\vec{q} = |\vec{q}| \left(0, \sin \theta_X, \cos \theta_X \right). \quad (\text{S33})$$

The polarized- X -emission rate with initial (final) polarization u (u') is given by

$$\Gamma_X^{u \rightarrow u'} = \frac{1}{2E_{n,k_3}} \sum_{n'=0}^n \sum_{s'=0}^{\infty} \int \frac{dk'_3}{(2\pi)} \frac{1}{2E_{n',k'_3}} \int \frac{d^3q}{(2\pi)^3} \frac{1}{2E_q} \left| \int d^3x M_{uu'}(r, \phi, z) \right|^2 (2\pi)^2 \delta(E_i - E_f - E_q) \delta(k_3 - k'_3 - |\vec{q}| \cos \theta_X) \quad (\text{S34})$$

Here $E_i = E_{n,k_3}$, $E_f = E_{n',k'_3}$, the sums are over $\{n', s'\}$, respectively, the final-state fermion Landau-level, and radial quantum numbers, and we have employed the energy and 3-momentum conservation of the problem to obtain the reduced matrix element for X -emission from electrons reads

$$M_{uu'}(r, \phi, z) = g_X \left(\bar{U}(n', s', k'_3, u') \tilde{O}_X \bar{U}(n, s, k_3, u) \right) \exp[i(\phi(\ell - \ell') - r|\vec{q}| \sin \theta_X \sin \phi)] \quad (\text{S35})$$

One performs the ϕ and subsequently the r integral using

$$\frac{1}{2\pi} \int_0^{2\pi} d\phi \exp[i(\phi(\ell - \ell') - r|\vec{q}| \sin \theta_X \sin \phi)] = J_{\ell - \ell'}(|\vec{q}| r \sin \theta_X) \quad (\text{S36})$$

$$\int_0^{\infty} (2\gamma) r dr J_{\ell - \ell'}(k r \sin \theta) \mathcal{I}_{n,s}(\rho) \mathcal{I}_{n',s'}(\rho) = \mathcal{I}_{n,n'}(\bar{x}) \mathcal{I}_{s',s'}(\bar{x}) \quad (\text{S37})$$

where we have used $\rho = \gamma r^2$ from Eq. (S19), and defined

$$\bar{x} = \frac{|\vec{q}|^2 \sin^2 \theta_X}{4\gamma} \quad (\text{S38})$$

In the transition rate, using the Lagurre-Gaussian's completeness relations, the only s' dependence then reads

$$\sum_{s'=0}^{\infty} (\mathcal{I}_{s',s'}(\bar{x}))^2 = 1 \quad (\text{S39})$$

The sum, $\sum_{n'=0}^n$, over final state fermion Landau-levels can be exchanged by an integral over the difference of initial and final levels, $\nu = n - n'$,

$$\sum_{n'=0}^n \rightarrow \int_0^n d\nu \quad (\text{S40})$$

In order to ease calculations, we choose a reference-frame in which $k_3 = 0$. Results for non-zero, k_3 can be obtained by boosting along the 3-direction. The initial and final state energies then read

$$E_i = \sqrt{m^2 + 4n\gamma}, \quad E_f = \sqrt{m^2 + 4(n - \nu)\gamma + |\vec{q}|^2 \cos^2 \theta_X}, \quad E_q = \sqrt{|\vec{q}|^2 + m_X^2} \quad (\text{S41})$$

and also

$$k'_3 = -|\vec{q}| \cos \theta_X \quad (\text{S42})$$

The ν -integral can be performed over the δ -function using

$$\frac{d}{d\nu} (E_i - E_f - E_q) = \frac{2\gamma}{E_f} \quad (\text{S43})$$

and using the solution

$$\nu = \frac{2E_i E_q - m_X^2 - |\vec{q}|^2 \sin^2 \theta_X}{4\gamma} \quad (\text{S44})$$

which, in turn, implies

$$m_X < E_q < E_i - m, \quad 0 < |\vec{q}| < \sqrt{(E_i - m)^2 - m_X^2} \equiv q_{\max} \quad (\text{S45})$$

Finally, the transition rate reads

$$\Gamma_X^{u \rightarrow u'} = \frac{1}{2\pi} \int_{-1}^1 d(\cos \theta_X) \int_0^{q_{\max}} d|\vec{q}| \frac{|\vec{q}|^2}{2E_q} \frac{E_f}{2\gamma} \left(\frac{|M_{uu'}|^2}{2E_i 2E_f} \right) \quad (\text{S46})$$

where Eq. (S37), S39, S41, S42, and S44 are assumed.

It is useful to perform a variable change which rescales the momentum integral to the $[0, \infty)$ domain,

$$y = \frac{1}{\xi_0} \frac{|\vec{q}|/E_i}{1 - |\vec{q}|/q_{\max}} \quad \Leftrightarrow \quad |\vec{q}| = E_i \frac{\xi_0 y}{1 + \xi_0 y E_i/q_{\max}} \quad (\text{S47})$$

where ξ_0 , defined in Eq. (7), is used, foreseeing a small parameter expansion. With $\xi_0 \ll 1$, and the small parameter expansions in next subsections, one finds several useful approximate expressions which are listed in Sec. VII.

When these results are put in correctly, it turns out that the only meaningful effect of the $m_X \neq 0$ is in the (phase-space) integrals over Bessel-K functions, while other effects in m_X/m , and m_X^2/E_i^2 are sub-leading. In the y , $\cos \theta_X$ variables, the X -emission rate can then be written as

$$\Gamma_X^{u \rightarrow u'} = \frac{27}{32\pi (m/E_i)^9 E_i \rho^2 \xi_0} \int_0^\infty dy \frac{y}{(1 + \xi_0 y)^4} \int_{-1}^1 d(\cos \theta_X) \left(\frac{|M_{uu'}^{\text{LO}}|^2}{4E_i E_f} \right) \quad (\text{S48})$$

where $M_{uu'}^{\text{LO}}$ stands for the leading order expansions described in the subsequent sub-sections¹¹

¹¹ for similar considerations, we approximate $E_i/q_{\max} \approx 1$. Note that we have kept the $E_i E_f$ factor in the ratio, due to our ‘‘particle-physics’’ normalization of the wave-functions.

B. Small Parameter Expansions of the Matrix Element

In a planner high-energy storage-ring, the particles are ultra-relativistic, $m \ll E_i$, and the emission of radiation therefore occurs close to the plane of the ring, at small $|\cos \theta_X|$. The kinematic variables can be expanded in

$$\epsilon_0 = 1 - \beta^2 = \frac{m^2}{E_i^2}, \quad \epsilon = 1 - \beta^2 \sin^2 \theta_X \quad (\text{S49})$$

which are the small parameters for the synchrotron case ($\cos^2 \theta_X = \frac{\epsilon - \epsilon_0}{1 - \epsilon_0}$). With the emission of a light X particle, there is another small parameter

$$\epsilon_x = \frac{m_X^2}{E_q^2} \approx \frac{m_X^2}{|\vec{q}|^2} \quad (\text{S50})$$

where $E_q = \sqrt{|\vec{q}|^2 + m_X^2}$, and $|\vec{q}|$ are the energy and momentum of the X particle, which is given as a solution to the equation

$$|\vec{q}|^2 = (E_i - Ef)^2 - m_X^2 = \left(\sqrt{m^2 + 4\gamma n} - \sqrt{m^2 + 4\gamma n + |\vec{q}|^2 \cos^2 \theta_X} \right)^2 - m_X^2 \quad (\text{S51})$$

The solution, and additional kinematic variables can be expanded in $\epsilon_0, \epsilon, \epsilon_X$ to give

$$|\vec{q}| \approx \sqrt{4\gamma} \left(\sqrt{n} - \sqrt{n'} \right) \left(1 - \epsilon \frac{\sqrt{n} - \sqrt{n'}}{2\sqrt{n'}} - \frac{\epsilon_0}{2} - \frac{\epsilon_X}{2} \right) \quad (\text{S52})$$

$$1 - \frac{\bar{x}}{x_0} \approx 1 - \frac{|\vec{q}|^2 \sin^2 \theta_X}{4\gamma \left(\sqrt{n} - \sqrt{n'} \right)^2} \approx \sqrt{\frac{n}{n'}} \epsilon + \epsilon_X \quad (\text{S53})$$

where x_0 is defined below in Eq. (S57). Similarly,

$$y = \frac{1}{\xi_0} \frac{|\vec{q}|/E_i}{1 - |\vec{q}|/q_{\max}} \approx \frac{4}{3} \epsilon_0^{3/2} n \sqrt{\frac{x_0}{n'}} \left(1 - \frac{\sqrt{n x_0} \epsilon}{n'} \frac{1}{2} - \left(1 + \sqrt{\frac{x_0}{n}} + \frac{x_0}{n} \right) \frac{\epsilon_X}{2} + \frac{x_0}{n'} \epsilon_0 \right) \quad (\text{S54})$$

and

$$\sqrt{\frac{n}{n'}} \approx \frac{E_i}{E_f} = (1 + \xi_0 y E_i / q_{\max}) \left(1 + \frac{m_X^2}{2E_i^2} \frac{1 + 2\xi_0 y}{\xi_0 y} \right) \quad (\text{S55})$$

C. WKB Approximation of The Lagurre Gaussians $\mathcal{I}_{n,n'}(x)$

In [4] an approximate form is derived for the Lagurre Gaussian functions, $\mathcal{I}_{n,n'}(x)$. Here we summarize the relevant results, and generalize them to the massive case. The differential equation for $\mathcal{I}_{n,n'}(x)$ is

$$\frac{d^2}{dx^2} \left(x^{1/2} \mathcal{I}_{n,n'}(x) \right) - f(x) x^{1/2} \mathcal{I}_{n,n'}(x) \quad (\text{S56})$$

where $f(x) = 0$ is solved by

$$\left. \begin{matrix} x \\ x' \end{matrix} \right\} = (n + n' + 1) \mp (4nn' + 2(n + n' + 1))^{1/2} \approx \left(n^{1/2} \mp n'^{1/2} \right)^{1/2} \quad (\text{S57})$$

and the approximation is for $n \gg 1, n' \gg 1$ (as would be appropriate when the Landau-level describes a macroscopic classical trajectory in the storage-ring).

Equation (S56) is a Schrödinger-like equation for $(x^{1/2} \mathcal{I}_{n,n'}(x))$. An approximate solution can be obtained close to the turning points of the potential $\{x_0, x'_0\}$ using the WKB method. Sokolov & Ternov [4] obtain

$$\left\{ \begin{array}{l} \mathcal{I}_{n,n}(x) = \frac{1}{\pi\sqrt{3}} \left(1 - \frac{x}{x_0} \right)^{1/2} K_{1/3}(z) \\ \mathcal{I}_{n,n}(x)' = \frac{(nn')^{1/4}}{\pi\sqrt{3}x_0} \left(1 - \frac{x}{x_0} \right) K_{2/3}(z) \end{array} \right. \quad \text{for } x = x_0 + 0^+ \quad (\text{S58})$$

where the 0^+ notation indicates that x is close to, but larger than x_0 , and

$$z = \frac{2}{3} (x_0^2 n n')^{1/4} \left(1 - \frac{x}{x_0}\right)^{3/2} \quad (\text{S59})$$

$$\mathcal{I}_{n,n'-1}(x) = \sqrt{\frac{x}{n'}} \left(\frac{n-n'-x}{2x} \mathcal{I}_{n,n}(x) - \mathcal{I}_{n,n'}(x)' \right) \quad (\text{S60})$$

$$\mathcal{I}_{n-1,n'}(x) = \sqrt{\frac{x}{n}} \left(\frac{n-n'+x}{2x} \mathcal{I}_{n,n}(x) + \mathcal{I}_{n,n'}(x)' \right) \quad (\text{S61})$$

$$\mathcal{I}_{n-1,n'-1}(x) = \frac{x}{\sqrt{n n'}} \left(\frac{n+n'+x}{2x} \mathcal{I}_{n,n}(x) - \mathcal{I}_{n,n'}(x)' \right) \quad (\text{S62})$$

Using the small parameter approximations of Sec. VB, we find

$$1 - \frac{x}{x_0} \approx \sqrt{\frac{n}{n'}} \left(\epsilon + \frac{n'}{n} \epsilon_X \right) = \sqrt{\frac{n}{n'}} \left(\epsilon + \frac{m_X^2}{E_i^2} \frac{1 + \xi_0 y}{(\xi_0 y)^2} \right) \quad (\text{S63})$$

$$z \approx \frac{1}{2} y \epsilon_0^{3/2} \left(\epsilon + \frac{n'}{n} \epsilon_X \right)^{3/2} = \frac{1}{2} y \epsilon_0^{3/2} \left(\epsilon + \frac{m_X^2}{E_i^2} \frac{1 + \xi_0 y}{(\xi_0 y)^2} \right)^{3/2} \quad (\text{S64})$$

so that

$$\begin{aligned} \begin{pmatrix} \mathcal{I}_{n,n'}(\bar{x}) \\ \mathcal{I}_{n,n'-1}(\bar{x}) \\ \mathcal{I}_{n-1,n'}(\bar{x}) \\ \mathcal{I}_{n-1,n'-1}(\bar{x}) \end{pmatrix} &= \frac{\sqrt{1 + \xi_0 y E_i / q_{\max}}}{\pi \sqrt{3}} \left(1 + \frac{m_X^2}{4E_i^2} \frac{1 + 2\xi_0 y}{\xi_0 y} \right) \left(\epsilon + \frac{m_X^2}{E_i^2} \frac{1 + \xi_0 y}{(\xi_0 y)^2} \right)^{1/2} \\ &\quad \begin{pmatrix} 0 \\ -(1 + \xi_0 y) \left(1 + \frac{m_X^2}{4E_i^2} \frac{1 + 2\xi_0 y}{\xi_0 y} \right) \\ 1 \\ -\xi_0 y - (1 + \xi_0 y) \frac{m_X^2}{4E_i^2} \frac{1 + 2\xi_0 y}{\xi_0 y} \end{pmatrix} \left(\epsilon + \frac{m_X^2}{E_i^2} \frac{1 + \xi_0 y}{(\xi_0 y)^2} \right)^{1/2} K_{2/3}(z) \end{pmatrix} \end{aligned} \quad (\text{S65})$$

VI. INTEGRAL EVALUATION

The Bessel-K functions we use as a result of the WKB approximation (Sec. VC) lead to angular integrals of the form

$$I(a, b, c, d) \equiv \int_{-1}^1 d \cos \theta \left(\epsilon + \frac{m_X^2}{E_i^2} \frac{1 + \xi_0 y}{(\xi_0 y)^2} \right)^a \cos^d \theta K_b(z) K_c(z) \quad (\text{S66})$$

where $a \in \{\frac{1}{2}, 1, \frac{3}{2}\}$, $b, c \in \{\frac{1}{3}, \frac{2}{3}\}$, d is a non-negative even integer, and z is given in Eq. (S64), and $\epsilon = (1 - \epsilon_0) \cos^2 \theta + \epsilon_0$ via Eq. (S49). The integrand in Eq. (S66) is an even function of $\cos \theta$ on the $[-1, 1]$ domain. In addition, the Bessel-K functions decay quickly for large arguments. The integral can then be approximated by evaluating the integral in the domain $[0, \infty)$, and multiplying by 2. This class of integrals has been evaluated in [85], with the results given as a recursion relation (see also [24], and [4]). We apply the prescription and obtain results for the case of massive particles. We define

$$\zeta \equiv \left(1 + \frac{1 + \xi_0 y}{(\xi_0 y)^2} \frac{m_X^2}{m^2} \right) \quad (\text{S67})$$

and find

$$I(1, \frac{1}{3}, \frac{1}{3}, 0) = \frac{2\pi}{\sqrt{3}y} \epsilon_0^{3/2} \int_y^\infty \zeta^{3/2} K_{1/3}(x) dx \quad (\text{S68})$$

$$I(1, \frac{1}{3}, \frac{1}{3}, 2) = \frac{\pi}{\sqrt{3}y} \epsilon_0^{5/2} \zeta \left(\int_y^\infty \zeta^{3/2} K_{5/3}(x) dx - K_{2/3}(y \zeta^{3/2}) \right) \quad (\text{S69})$$

$$I(1, \frac{1}{3}, \frac{1}{3}, 4) = \frac{\pi}{2\sqrt{3}y^2} \epsilon_0^{7/2} \zeta^{1/2} \left(K_{1/3}(y \zeta^{3/2}) - \frac{3y}{2} \zeta^{3/2} \left(\int_y^\infty \zeta^{3/2} K_{5/3}(x) dx - K_{2/3}(y \zeta^{3/2}) \right) \right) \quad (\text{S70})$$

$$I(2, \frac{2}{3}, \frac{2}{3}, 0) = \frac{\pi}{\sqrt{3}y} \epsilon_0^{5/2} \zeta \left(\int_y^\infty \zeta^{3/2} K_{5/3}(x) dx + K_{2/3}(y \zeta^{3/2}) \right) \quad (\text{S71})$$

$$I(2, \frac{2}{3}, \frac{2}{3}, 2) = \frac{\pi}{6\sqrt{3}y^2} \epsilon_0^{7/2} \left(5\zeta^{1/2} K_{1/3}(y \zeta^{3/2}) + \frac{3y}{2} \zeta^2 \left(\int_y^\infty \zeta^{3/2} K_{1/3}(x) dx - K_{2/3}(y \zeta^{3/2}) \right) \right) \quad (\text{S72})$$

$$I(\frac{3}{2}, \frac{1}{3}, \frac{2}{3}, 0) = \frac{2\pi}{\sqrt{3}y} \epsilon_0^2 \zeta^{1/2} K_{1/3}(y \zeta^{3/2}) \quad (\text{S73})$$

$$I(\frac{3}{2}, \frac{1}{3}, \frac{2}{3}, 2) = \frac{2\pi}{3\sqrt{3}y^2} \epsilon_0^3 \int_y^\infty \zeta^{3/2} K_{1/3}(x) dx \quad (\text{S74})$$

$$(\text{S75})$$

In presenting our results, we follow [4] and use the relation

$$K_{1/3}(\alpha) + K_{5/3}(\alpha) = -2 \frac{d}{d\alpha} K_{2/3}(\alpha) \quad (\text{S76})$$

VII. USEFUL EXPANSIONS OF KINEMATIC VARIABLES

Some useful expansions

$$|\vec{q}| = E_i \frac{\xi_0 y}{1 + \xi_0 y E_i / q_{\max}} \quad (\text{S77})$$

$$E_f = E_i \frac{1}{1 + \xi_0 y E_i / q_{\max}} \left(1 - \frac{m_X^2}{2E_i^2} \frac{1 + 2\xi_0 y}{\xi_0 y} \right) \quad (\text{S78})$$

$$\frac{k'_3}{E_f} = -\xi_0 y \cos \theta_X \left(1 + \frac{m_X^2}{2E_i^2} \right) \quad (\text{S79})$$

$$\sqrt{1 - \frac{k'^2_3}{E_f^2}} = 1 - \frac{1}{2} (\xi_0 y)^2 \cos^2 \theta_X \left(1 + \frac{m_X^2}{2E_i^2} \right) \quad (\text{S80})$$

$$E_f^2 - k'^2_3 = \left(\frac{E_i}{1 + \xi_0 y E_i / q_{\max}} \right)^2 \left(1 - \frac{m_X^2}{E_i^2} \frac{1 + 2\xi_0 y}{\xi_0 y} - (\xi_0 y)^2 \cos^2 \theta_X \right) \quad (\text{S81})$$

$$\frac{E_i}{q_{\max}} \approx 1 + \frac{m}{E_i} + \frac{m_X^2}{2E_i^2} \quad (\text{S82})$$

$$(\text{S83})$$

VIII. SPIN-1 POLARIZATION VECTORS

The transverse and longitudinal polarization vectors for spin-1 are

$$(\varepsilon^T)_\mu^{\chi=\pm} = \frac{1}{\sqrt{2}} \left(0, 1, i\chi \cos \theta_X, -i\chi \sin \theta_X \right) \quad (\text{S84})$$

$$(\varepsilon^L)_\mu = \left(\frac{|\vec{q}|}{m_X}, 0, \frac{E_q}{m_X} \sin \theta_X, \frac{E_q}{m_X} \cos \theta_X \right) \quad (\text{S85})$$

IX. FULL RESULTS OF SPIN-FLIP TRANSITION RATES

The spin-flip transition-rate by X -emission,

$$\Gamma_X^{\text{sf}}(u) \equiv \Gamma_H(e^-(u) \rightarrow e^-(-u)\gamma). \quad (\text{S86})$$

depends on the initial spin state of the fermion, $u = +1, -1$ for "up" and "down" respectively. The emitting state is an electron of mass m , and energy E_i , and the bending radius is R . We define

$$y = \frac{1}{\xi_0} \frac{|\vec{q}|/E_i}{1 - |\vec{q}|/q_{\text{max}}} \quad (\text{S87})$$

$$\zeta \equiv \left(1 + \frac{1 + \xi_0 y}{(\xi_0 y)^2} \frac{m_X^2}{m^2} \right) \quad (\text{S88})$$

$$\mathcal{K} \equiv \int_y^\infty dx K_{5/3}(x), \quad \bar{\mathcal{K}} \equiv \int_y^\infty dx K_{1/3}(x), \quad (\text{S89})$$

$$K_{1/3} \equiv K_{1/3}(y\zeta^{3/2}), \quad K_{2/3} \equiv K_{2/3}(y\zeta^{3/2}) \quad (\text{S90})$$

The rates for the various X are given by

$$\frac{d\Gamma_{V_T}^{\text{sf}}}{dy} = g_V^2 \frac{\sqrt{3}E_i}{2^5\pi^2 m\rho} \left(\frac{1}{(1 + \xi_0 y)^2} \frac{m_V^2}{m^2} \mathcal{K} + \frac{2(\xi_0 y)^2}{(1 + \xi_0 y)^3} (K_{2/3} + u\zeta^{1/2}K_{1/3}) \right) \quad (\text{S91})$$

$$\frac{d\Gamma_{V_L}^{\text{sf}}}{dy} = g_V^2 \frac{\sqrt{3}E_i}{2^5\pi^2 m\rho} \left(\frac{m^2 m_V^2}{16E_i^4} \right) \frac{(\xi_0 y)^2}{1 + \xi_0 y} \left(\left(2\zeta - \frac{\zeta^{1/2}}{2} - \frac{8u}{3y} \right) \mathcal{K} + \left(-2\zeta + \frac{\zeta^{1/2}}{2} + \frac{16u}{3y} \right) K_{2/3} + \frac{5\zeta^{1/2}}{3y} K_{1/3} \right) \quad (\text{S92})$$

$$\frac{d\Gamma_{A_T}^{\text{sf}}}{dy} = g_A^2 \frac{\sqrt{3}E_i}{2^5\pi^2 m\rho} \left(\frac{(2 + \xi_0 y)^2}{(1 + \xi_0 y)^2 (\xi_0 y)^2} \frac{m_A^2}{m^2} \mathcal{K} + \frac{2(2 + \xi_0 y)^2}{(1 + \xi_0 y)^3} (K_{2/3} + u\zeta^{1/2}K_{1/3}) \right) \quad (\text{S93})$$

$$\begin{aligned} \frac{d\Gamma_{A_L}^{\text{sf}}}{dy} &= g_A^2 \frac{\sqrt{3}E_i}{2^5\pi^2 m\rho} \left(\left(\frac{m^2}{m_A^2} \frac{(\xi_0 y)^2}{(1 + \xi_0 y)^3} \right) \left((\zeta - 2)\mathcal{K} + (4 + \zeta)K_{2/3} + 4u\zeta^{1/2}K_{1/3} \right) \right. \\ &\quad \left. + 2 \frac{m_A^2}{m^2} \frac{1}{(\xi_0 y)^2 (1 + \xi_0 y)} \bar{\mathcal{K}} - \frac{4u\zeta^{1/2}}{(1 + \xi_0 y)^2} K_{1/3} \right) \quad (\text{S94}) \end{aligned}$$

$$\frac{d\Gamma_S^{\text{sf}}}{dy} = g_S^2 \frac{\sqrt{3}E_i}{2^5\pi^2 m\rho} \left(8 \frac{(\xi_0 y)^2}{(1 + \xi_0 y)^3} \zeta \right) (\mathcal{K} + K_{2/3}) \quad (\text{S95})$$

$$\frac{d\Gamma_a^{\text{sf}}}{dy} = g_a^2 \frac{\sqrt{3}E_i}{2^5\pi^2 m\rho} \left(\frac{(\xi_0 y)^2}{(1 + \xi_0 y)^3} \right) \left((\zeta - 2)\mathcal{K} + (4 + \zeta)K_{2/3} + 4u\zeta^{1/2}K_{1/3} \right) \quad (\text{S96})$$

where for the massive vector, and axial-vector cases we distinguish between the transverse, and longitudinal modes, denoting them by T , and L respectively.

The result of Sec. IV B are obtained by taking the limit $\frac{m_X}{m\xi_0} \rightarrow 0$, (or $\zeta \rightarrow 1$). In this limit, the order of the y and x integrals can be interchanged with explicit expression for the limits, and the integrals are straightforward to perform after an expansion in ξ_0 .